A

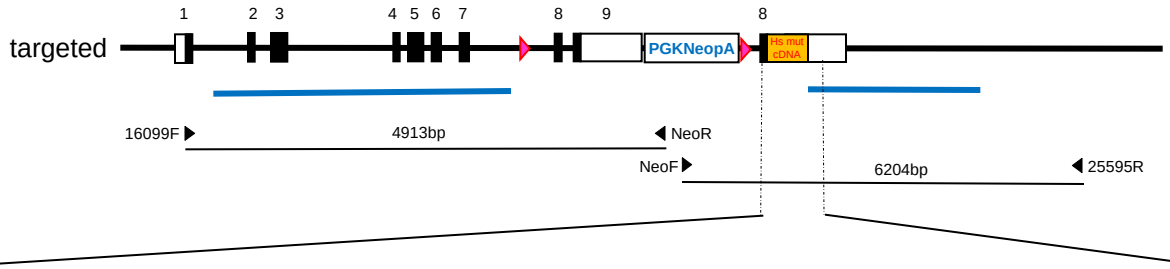

5′-gtcaagtccgggacaatctttgacaatttcctcatcaccaatgatgaggcctatgcagaggagtttgGCAACGAG
ACGTGGGGCGTAACAAAGGCAGCAGAGAAACAAATGAAGGACAAACAGGACGAGGAGCAGAGGACAAGGAGGATGATG
AGGACAAAGATGAGGATGAGGAGGATGAGGAGGACAAGGAGGAAGATGAGGAGGAAGATGTCCCCGGCCAGGCCAAGG
ACGAGCTGTAGAGAGGCCTGCCTCCAGGGCTGGACTGAGGCCTGAacaccctgccgcagagctggctgctcccaataa
tgtctctatgagactcaagaacttttcatttttccaggcaggttcagatctggggtagattctgattttgttcccct
gcctcccccattaccccccccctttttttttttactggtgtttgtctttaattctccttcagccctcatctggtttc-3′

B

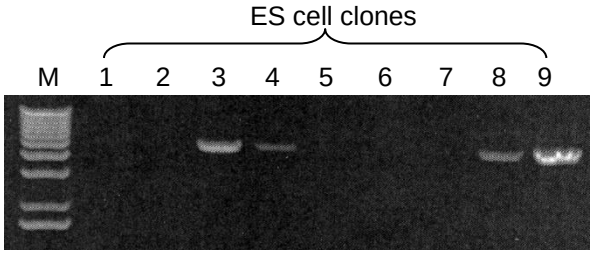

5’ long range PCR (16099F/NeoR)

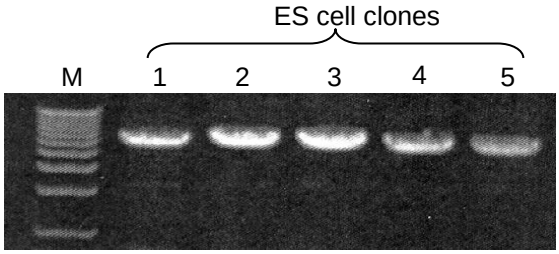

3’ long range PCR (NeoF/25595R)

C

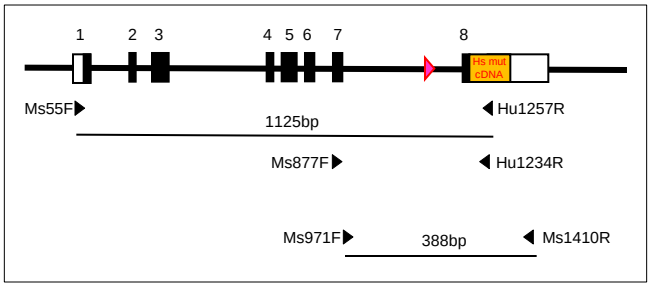

D

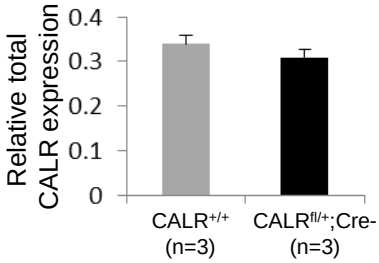

Supplemental Figure 1

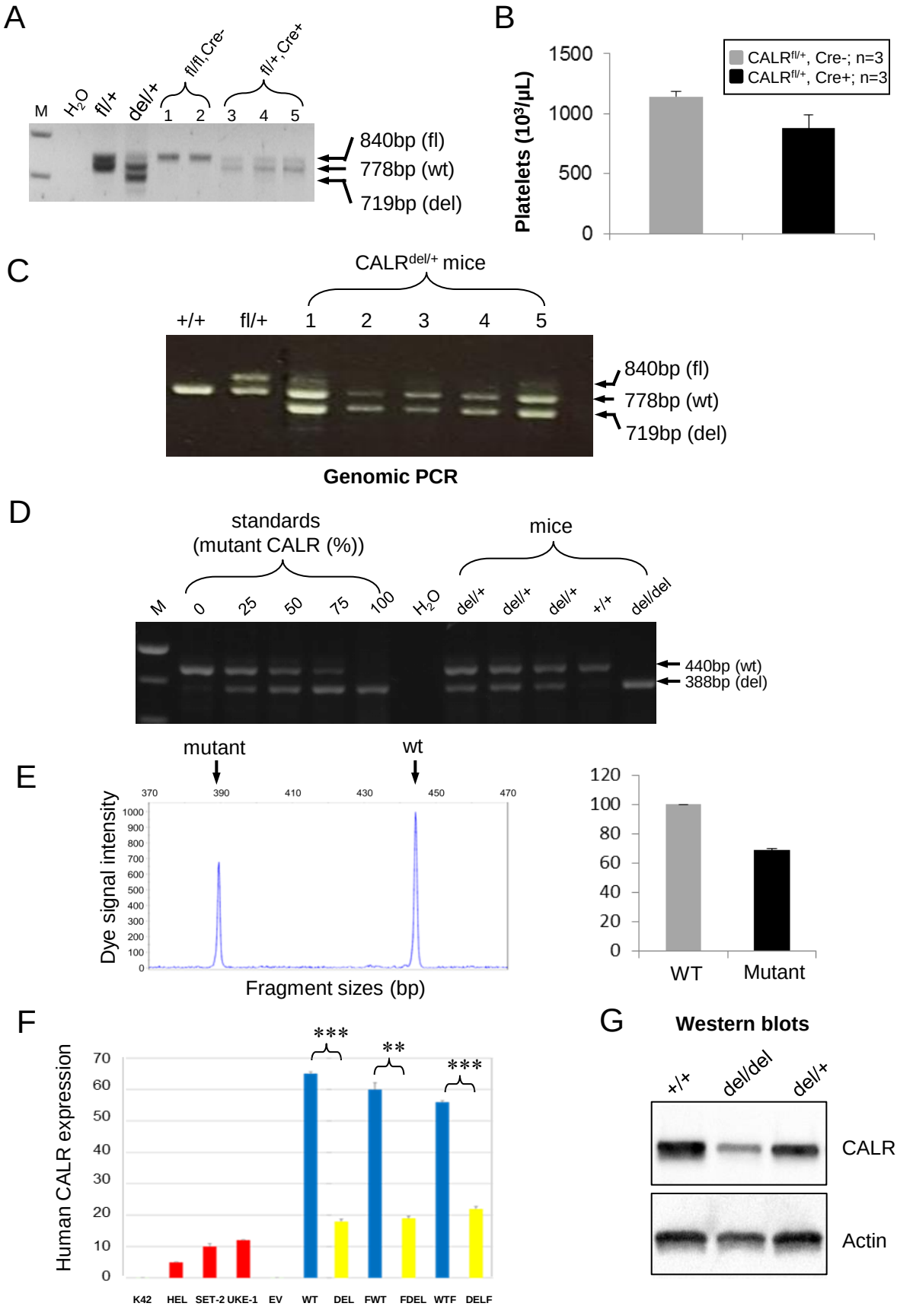

Supplemental Figure 2

A

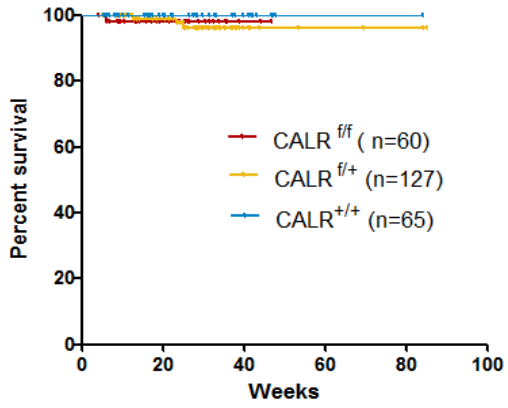

B

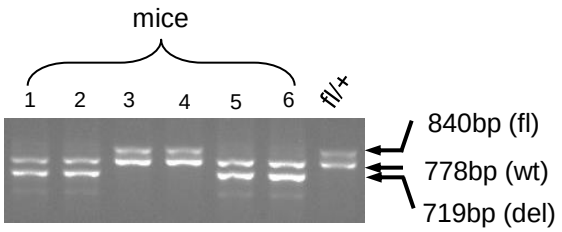

C

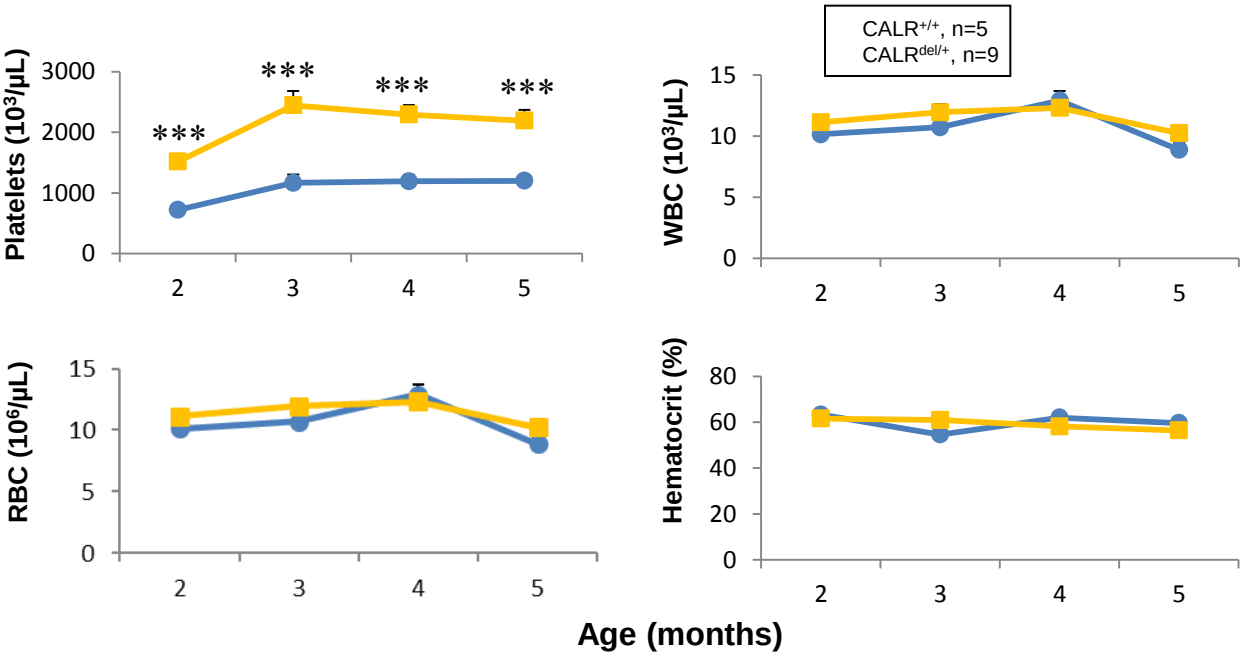

D

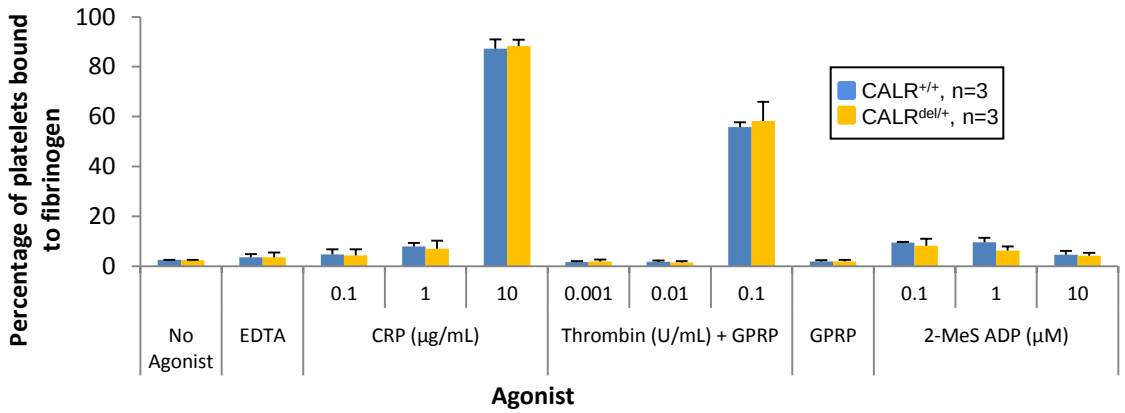

Supplemental Figure 3

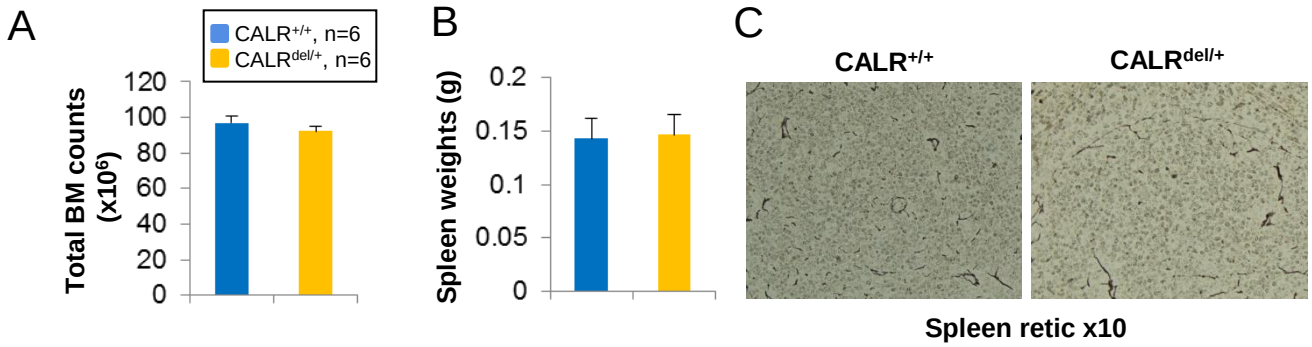

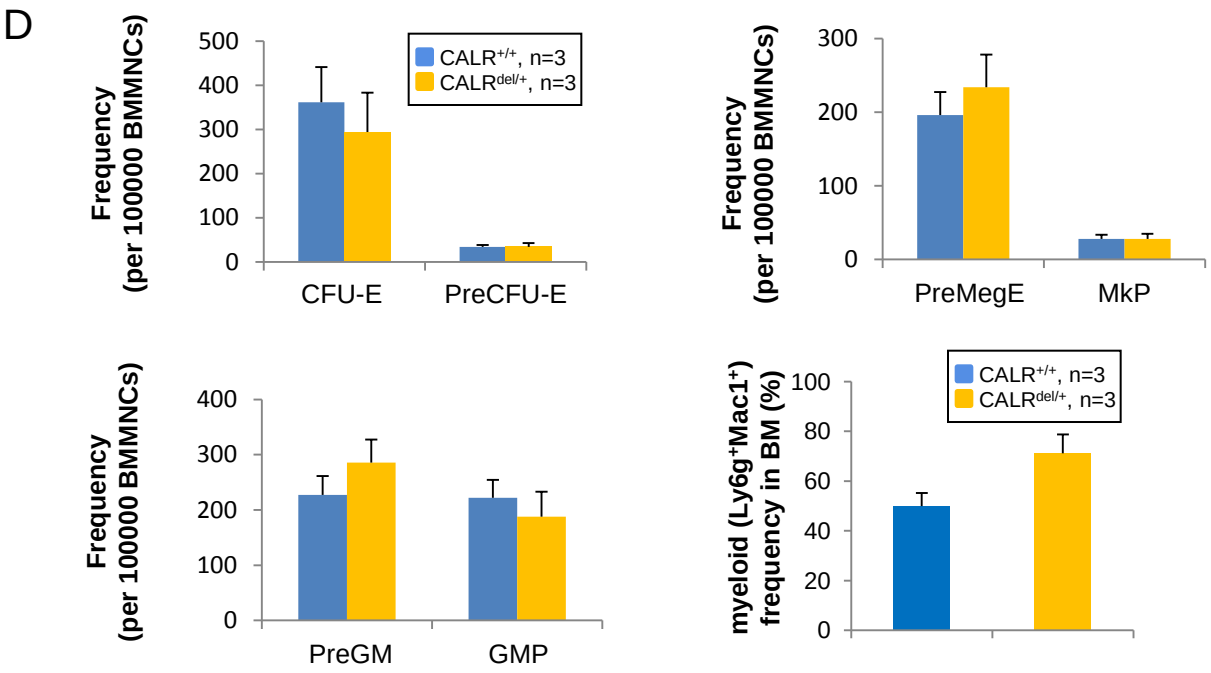

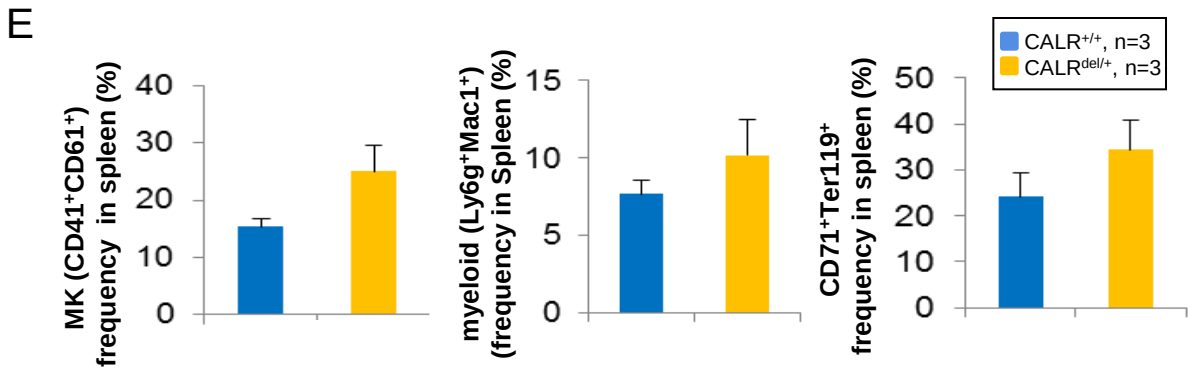

Supplemental Figure 4

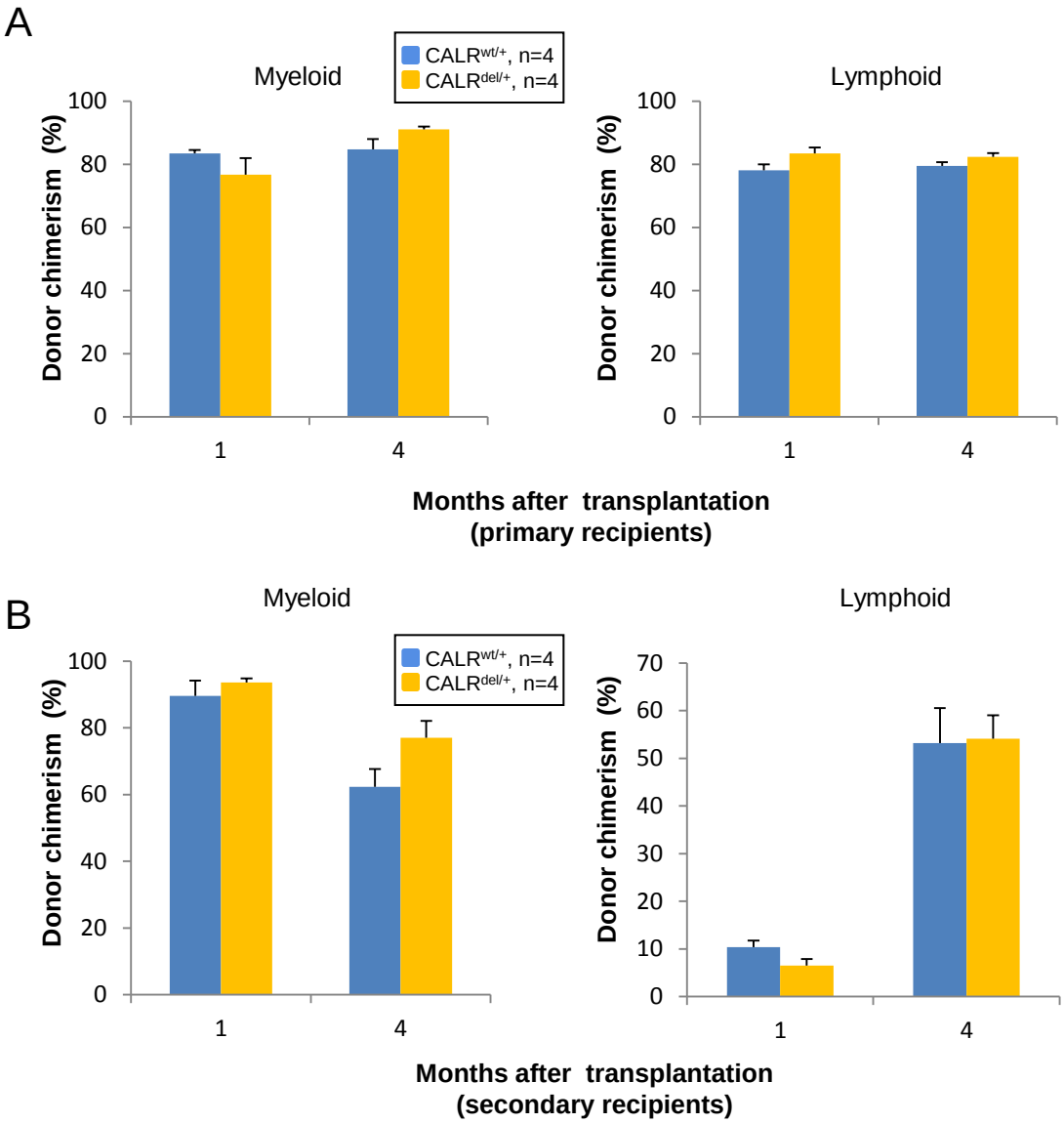

Supplemental Figure 5

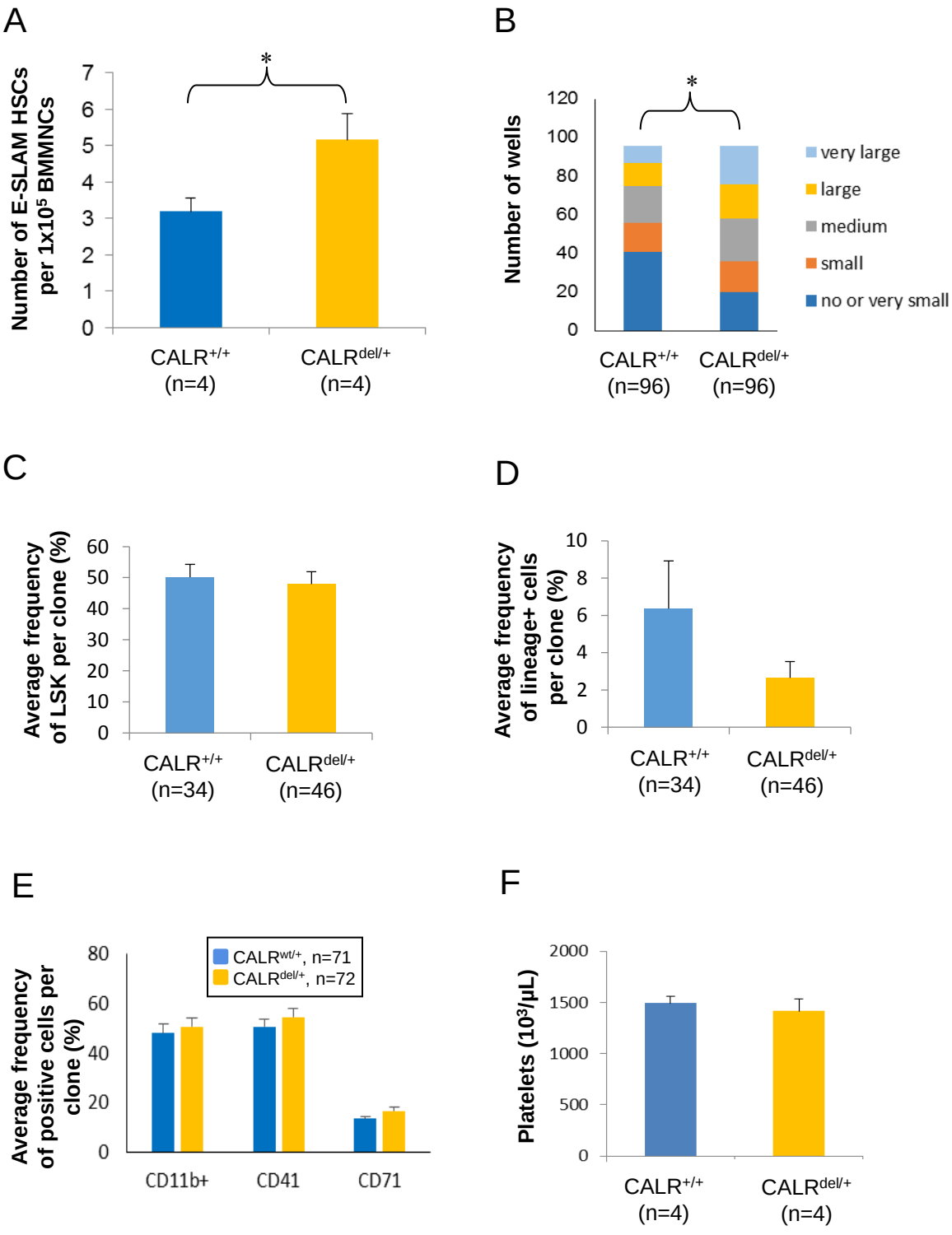

Supplemental Figure 6

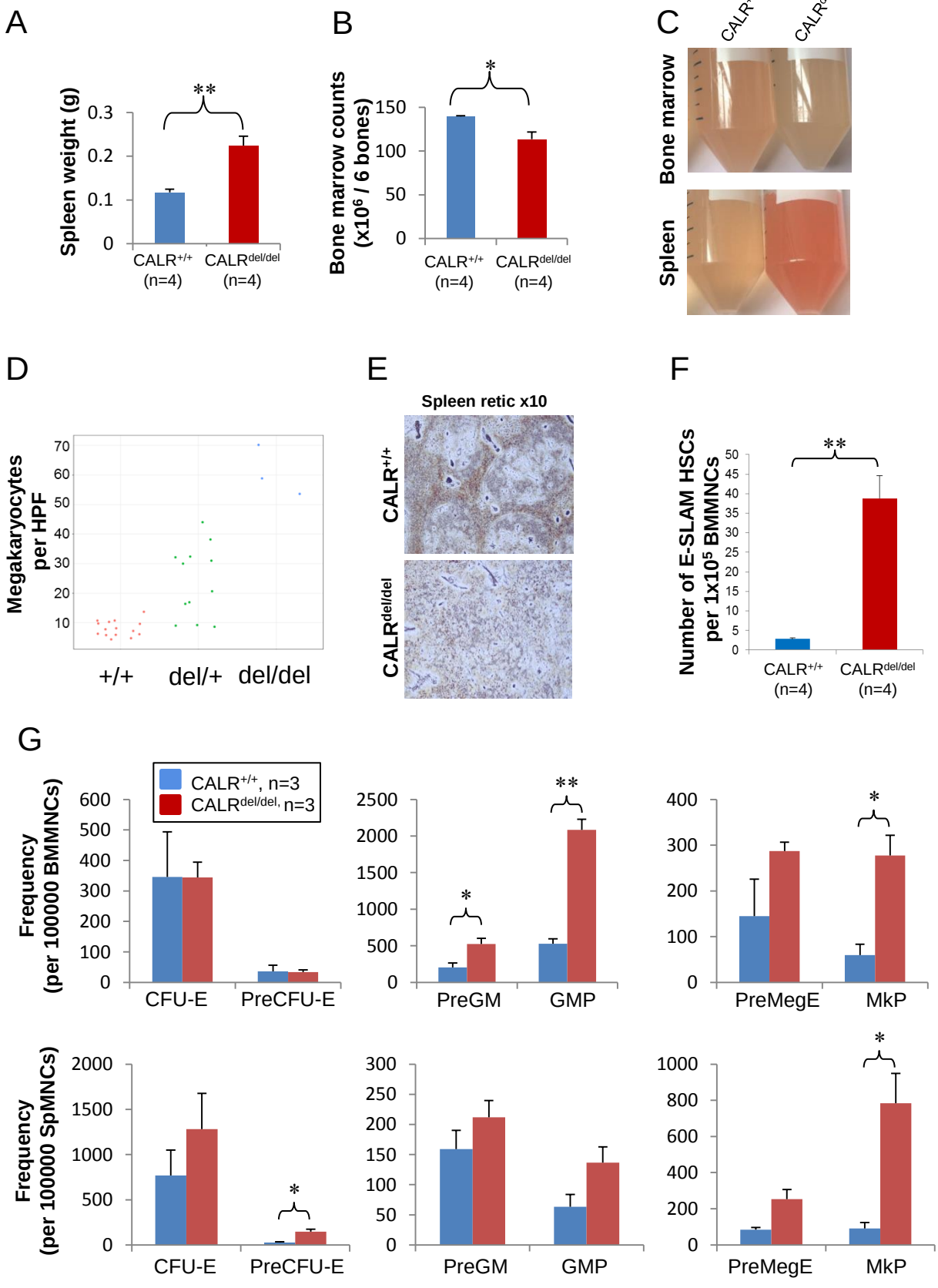

Supplemental Figure 7

SUPPLEMENTAL FIGURE LEGENDS

Supplemental Figure 1. Generation of a conditional humanized mutant CALR knock-in mouse model. (A) Diagrams showing the targeted allele. Homology arms in the targeting vector are shown in blue lines; long range PCR genotyping schemes with location of the primers and the product sizes indicated. Detailed nucleotide sequences of the mouse CALR exon 8 fused to human mutant 3'cDNA are shown; the mutant stop codon TGA is underlined. (B) Characterization of ES cell targeting. Long range PCR was performed on genomic DNA from ES clones using primers 16099F and NeoR for detecting 5' homologous recombination (left panel). M, DNA marker; lanes 1-9, ES clones. ES clones that were positive for 5' homologous recombination were analysed using long range PCR with primers NeoF and 25595R for detecting 3' homologous recombination (right panel). M, DNA marker; lanes 1-5, ES clones. (C) Characterization of knock-in alleles after Cre recombination. Diagram showing schemes of RT-PCR analysis with product size, location of the RT-PCR primers and the sequencing primers indicated. (D) Analysis of wildtype CALR expression from the targeted allele. Quantitative RT-PCR was performed to assess total CALR expression in mice ($CALR^{fl/+}$, Cre-) compared with levels in mice with alleles of $CALR^{+/+}$. Bar graphs show relative CALR expression to Gapdh. Data are shown as mean ± SEM.

Supplemental Figure 2. Characterization of CALR mutant allele expression. (A) Analysis of recombination prior to pIpC treatment. Genomic PCR was performed on nucleated peripheral blood and showed no detectable Cre recombination in the mice analysed. M, DNA marker; fl/+, control DNA from targeted ES cells; del/+, DNA from ES cells carrying recombined allele (del); lanes 1-2, DNA from mice with homozygous floxed

alleles (fl); lanes 3-5, DNA from mice ($CALR^{fl/+}$, Cre+) prior to pIpC treatment. (B) Platelets counts were normal in mice ($CALR^{fl/+}$, Cre+) prior to pIpC treatment. (C) Analysis of Mx1Cre induced recombination. Genomic PCR was performed on nucleated peripheral blood from $CALR^{del/+}$ mice at 6 weeks after pIpC injection. +/+, control DNA from wild type mice; fl/+, DNA from floxed mice without Mx1Cre; lanes 1-5, DNAs from $CALR^{del/+}$ mice. (D) Analysis of mutant CALR expression in mice. Semi-quantitative RT-PCR was performed using BMMNCs from $CALR^{del/+}$ mice using primers Ms971F (located in mouse exon 7) and Ms1410R (located in 3'UTR of the mouse CALR). M, DNA marker; standards, mixed templates reflecting mol ratios of RT-PCR products from the wildtype and mutants CALR transcripts, i.e. 50% means 1 to 1 mol ratio; mice, three $CALR^{del/+}$ with one $CALR^{+/+}$ and one $CALR^{del/del}$ mice as controls. (E) Fragment analysis shows transcript levels of mutant CALR were lower relative to transcript from the WT allele. PCR was performed on cDNAs of HSPCs (Lin^{-} $Sca\text{-}1^{+}$ $cKit^{+}$) from six heterozygous mice to quantitate mutant CALR expression. A representive plot is shown with heights of vertical peaks representing dye signal intensity and horizontal positions of peaks reflecting the fragment size of the PCR amplicons. Bar graph shows relative levels of WT and mutant CALR alleles (WT levels normalized to 100). (F) Human mutant CALR transcript levels were lower than the wildtype controls. K42 (CALR deficient) cells[1] were transduced with multiple human CALR expression constructs respectively (untagged versions of calreticulin (WT and DEL), N-terminus FLAG-tagged (FWT and FDEL) and C-terminus FLAG-tagged (WTF and DELF). Stable cell lines were obtained and quantitative RT-PCR was performed to assess CALR expression. Relative CALR expression to ABL is shown. CALR transcript levels were also shown for several hematological cell lines such as HEL (erythroid) and SET2 and UKE-1

(megakaryocytic). **, p<0.01; ***, p<0.001; data were from triplicates and are shown as mean ± SEM. (G) Analysis of CALR protein by Western blots. Protein lysates from spleen cells from $CALR^{+/+}$, $CALR^{del/+}$ and $CALR^{del/del}$ mice were analysed using antibody detecting total CALR.

Supplemental Figure 3. Characterization of CALR mutant mice. (A) Mutant CALR expression in mice does not affect survival. Kaplan Meier analysis showed that both $CALR^{del/+}$ and $CALR^{del/del}$ mice have normal survival compared to WT controls. (B) Analysis of VavCre induced recombination. Genomic PCR was performed on nucleated peripheral blood from $CALR^{del/+}$ mice at 6-8 weeks of age. Lanes 1-6, DNAs from mice including four $CALR^{del/+}$ mice ($CALR^{fl/+}$, VavCre-; lanes 1, 2, 5 and 6) and two control mice ($CALR^{fl/+}$, VavCre-; lanes 3 and 4); fl/+, floxed allele control DNA from targeted ES cells. (C) $CALR^{del/+}$ mice induced by VavCre develop thrombocytosis. Time course of blood parameters showed significantly increased platelets but normal red cell parameters in the $CALR^{del/+}$ mice. * $P < 0.05$; *** $P < 0.001$; mean ± SEM are shown. (D) Platelets from $CALR^{del/+}$ mice did not show significantly altered response to CRP, thrombin and ADP. Flow cytometry was performed on whole blood to assess fibrinogen binding of platelets in response to the agonists.

Supplemental Figure 4. Progenitor and lineage analysis of $CALR^{del/+}$ mice. (A) Bone marrow cellularity is not altered in $CALR^{del/+}$ mice. Bar graph showing bone marrow cell counts per 6 bones from $CALR^{del/+}$ mice were similar to the control mice. (B) $CALR^{del/+}$ mice do not show splenomegaly. Bar graph showing weight of spleen from $CALR^{del/+}$ mice

was similar to the control mice. (C) $CALR^{del/+}$ mice do not show fibrosis in spleen. Silver staining of spleen sections showed no increased fibrosis in $CALR^{del/+}$ mice at 3-4 months after pIpC injection. (D) $CALR^{del/+}$ mice show no significant myeloerythroid expansion in bone marrow. Flow cytometry was performed to assess frequency of bone marrow myeloerythroid precursors and mature myeloid populations. (E) $CALR^{del/+}$ mice do not show significant changes in the frequency of MK, myeloid and erythroblasts in the spleen. Flow cytometry was performed to assess the frequency of megakaryocytes (MK, $CD41^{+}CD61^{+}$), myeloid ($Ly6g^{+}Mac1^{+}$) and erythroblasts ($CD71^{+}Ter119^{+}$). Data are shown as mean ± SEM.

Supplemental Figure 5. Thrombocytosis in $CALR^{del/+}$ mice is transplantable. (A) Bone marrow cells from $CALR^{del/+}$ mice exhibit comparable repopulating capacity to both myeloid and lymphoid repopulation in peripheral blood in primary non-competitive transplantation recipients. Donor chimerism was assessed using flow cytometry with antibodies for CD45.1 and CD45.2 to distinguish donor origin and is presented as percentage of $CD45.2^{+}$ cells. Antibodies for Ly6g and Mac1 were used for myeloid, B220 and CD3e for lymphoid lineages. (B) $CALR^{del/+}$ bone marrow cells exhibit comparable repopulating capacity to both myeloid and lymphoid repopulation in peripheral blood in secondary non-competitive transplantation recipients. Flow cytometry was performed as above; data are shown as mean ± SEM.

Supplemental Figure 6. Mutant CALR increases phenotypic HSCs which exhibit altered behavior in single cell *in vitro* analysis. (A) E-SLAM HSCs numbers are increased in $CALR^{del/+}$ mice. Flow cytometry was performed to assess the frequency of E-SLAM

HSCs ($CD45^+CD150^+CD48^-EPCR^+$) in the bone marrow of $CALR^{del/+}$ mice at 3-4 months post pIpC. *, $p<0.05$; p-value was calculated by a two-tailed, paired student's t-test; data are shown as mean ± SEM. (B) E-SLAM HSCs from $CALR^{del/+}$ mice form larger clones *in vitro*. After seven days of culture, clones derived from each single E-SLAM HSC were examined and scored visually for size. Clones were classified as no clone or very small (fewer than 50 cells), small (up to 100 cells), medium (ca. 250 cells), large (ca. 500 cells), or very large (ca. 2k cells), with numbers having been calculated from flow cytometry analysis. A chi-squared test was performed to compare differences in clone sizes between clones arising from $CALR^{del/+}$ and control E-SLAMs HSCs. *, $p<0.05$. (C) LSK frequency in clones derived from single HSCs of $CALR^{del/+}$ mice is not altered *in vitro*. After 7 days in culture, individual clones derived from single HSCs were analysed for LSK frequency using flow cytometry with antibodies for lineage cocktail, Sca-1 and c-Kit. (D) Frequency of lineage positive cells in clones derived from single HSCs of $CALR^{del/+}$ mice is not altered *in vitro*. After 7 days in culture, individual clones derived from single HSCs were analyzed using flow cytometry as in (C) and the frequency of lineage positive cells per clone was analysed. (E) Lineage differentiation is not affected in a single HSC *in vitro* assay. After 14 days in culture, individual clones were analyzed using flow cytometry with antibodies for Mac1, CD41 and CD71 to assess differentiation to myeloid, megakaryocytic and erythroid cells respectively. A total of 71 (WT) or 72 ($CALR^{del/+}$) clones were analyzed from six separate mice. Data are shown as mean ± SEM. (F) Competitive transplant recipients that received bone marrow from $CALR^{del/+}$ mice did not show increased platelet counts. Data are shown as mean ± SEM.

Supplemental Figure 7. **Homozygosity for CALR mutation ($CALR^{del/del}$) results in extreme thrombocytosis and development of myelofibrosis.** (A) $CALR^{del/del}$ mice develop splenomegaly. (B) $CALR^{del/del}$ mice bone marrow cellularity is reduced. Bar graphs show bone marrow cell counts per 6 bones from $CALR^{del/del}$ mice were significantly lower than the control mice. (C) $CALR^{del/del}$ mice develop extramedullary hematopoiesis in spleen. Pictures show that macroscopically, bone marrow specimens from the $CALR^{del/del}$ were paler and their spleen cell samples were redder. (D) $CALR^{del/del}$ mice show strikingly increased numbers of megakaryocytes in bone marrow. Megakaryocytes were visualized by histology and counted throughout 10 high-power fields (hpf, ×40 objective) per section. (E) $CALR^{del/del}$ mice show no increased fibrosis in spleen. Silver staining for reticulin of spleen sections showed no increased fibrosis in $CALR^{del/del}$ mice. (F) Numbers of E-SLAM HSC are markedly expanded in $CALR^{del/del}$ mice. Flow cytometry was performed to assess the frequency of E-SLAM HSCs ($CD45^{+}CD150^{+}CD48^{-}EPCR^{+}$) of $CALR^{del/+}$ mice at 3-4 months post pIpC. *, $p<0.05$; **, $p<0.01$; ***, $p<0.001$; data are shown as mean ± SEM. (G) $CALR^{del/del}$ mice show significant myeloerythroid expansion. Flow cytometry was performed to assess frequency of myeloerythroid precursors. *, $p<0.05$; **, $p<0.01$; data are shown as mean ± SEM.

1. Nakamura K, Bossy-Wetzel E, Burns K, et al. Changes in endoplasmic reticulum luminal environment affect cell sensitivity to apoptosis. *J Cell Biol*. 2000;150(4):731-740.

SUPPLEMENTAL METHODS

Genomic PCR for characterization of targeted alleles

Long-range PCRs were performed on genomic DNA from ES clones. The long range PCR was performed using a forward primer 16099F (5'-GCCTCGTCGTGTGTAATGTAA-3') and a reverse primer NeoR (5'-TCCAGACTGCCTTGGGAAAA-3') to detect 5' homologous recombination. ES clones that were positive for 5' homologous recombination were subjected to further long range PCR analysis using a forward primer NeoF (5'-TGGGAAGACAATAGCAGGCA-3') and a reverse primer 25595R (5'-GGGTCAAGGTGAAGGTCAGA-3') to confirm 3' homologous recombination. Long-range PCRs were also performed on genomic DNA from germline mice to confirm transmission of targeted alleles. All long-range PCRs were performed using Phusion hot start II PCR kit according to the manufacturer's instructions (Thermo Fisher Scientific).

Conventional PCR was performed routinely on ear notch DNA using forward primer F (5'-CCTACCTTCTCAGTGCATCAA-3'), reverse primer R (5'-ATCTGAACCTGCCTGGAAAA-3') and the KAPA2G fast ready mix PCR kit (Kapa Biosystems). This PCR detects wildtype, targeted and recombined alleles.

Induction of mutant CALR expression

Mice with interferon inducible recombinase (Mx1Cre) were bred with the $CALR^{fl/+}$ germline mice to allow the expression of the humanized mutant CALR in the hematopoietic system. 6-8 week-old mice were injected intraperitoneally with sterile polyinosinic-polycytidylic acid (pIpC) (Sigma-Aldrich, Dorset, UK) to induce Cre recombinase expression. Cohorts of

mice including $CALR^{fl/+}$ $Mx1Cre^{+}$ and littermate controls ($CALR^{+/+}$ $Mx1Cre^{+}$, $CALR^{+/+}$ $Mx1Cre^{-}$ or $CALR^{fl/+}$ $Mx1Cre^{-}$) were injected with 100μL pIpC (2.5 mg/mL in PBS, 250μg/dose) every other day for a total of 3 injections.

Total RNA extraction and cDNA synthesis

Total RNA was extracted from mouse bone marrow or ES cells using direct-zol RNA miniprep plus kit according to manufacturer's instruction (Zymo Research) and cDNA was synthesized using SuperScript® III First-Strand Synthesis System with random hexamers (Invitrogen).

RT-PCR analysis of mutant CALR mRNA expression

RT-PCR was performed on cDNA using KAPA2G fast ready mix PCR kit with forward primer Ms971F (5'-CTGTACTGGGCCTAGATCTCTG-3', located in the mouse CALR exon 7) and reverse primer Ms1410R (5'-ATCTGAACCTGCCTGGAAAA-3', located in the mouse CALR 3'UTR). RT-PCR was also performed using forward primer Ms55F (5'-TCGGT GCCGCTCCTGCTTGG-3', located in exon 1 of the mouse CALR and upstream of the 5' homology arm of the targeting vector) and a reverse primer Hu1257R (5'-TGAGGATGAGGAG GATGAGG-3', located in the human CALR sequence). PCR was performed using Phusion hot start II PCR kit (Thermal Fisher) and the RT-PCR product was cloned then subjected to Sanger sequencing using primers Ms877F (5'-GACAACCCAGATTACAAGGG-3') and Hu1234R (5'-CAAGGAGGATGATGAGGACAA-3'). Quantitative RT-PCR was performed using KAPA SYBR® FAST qPCR master mix (Sigma Aldrich) for total mouse CALR expression with

forward primer MsCALRqF1 (5'-TCCCCCGATGCAAATATCTA-3') and reverse primer MsCALRqR1 (5'-CTTGGTAACACCCCACGTCT-3'). Human CALR expression was assessed using quantitative RT-PCR using Taqman primers for CALR and ABL control purchased from Thermo Fisher.

Fragment analysis

RT-PCR was performed on isolated HSCPs (LSKs) using 6-FAM labelled forward primer 5'-GACAACCCAGATTACAAGGG-3' and reverse primer 5'-GGCCTCAGTCCAGCCCTG-3'. The PCR fragments were analysed using the 96-capillary 3730xl DNA Analyzer and the data plots were obtained using GeneMapper® allele calling software (Applied Biosystems). Levels of CALR transcript from wildtype allele was normalized to 100.

Blood and tissue histological analysis

Peripheral blood was collected from tail veins into EDTA-coated tubes every 4-6 weeks and automated total and differential blood cell counts were determined using a Woodley ABC blood counter (Woodley, Bolton, UK). For histological analysis, bone and spleen specimens were collected into 4% buffered formaldehyde (CellPath PLC, Powys, UK). Bones were decalcified in 25mM EDTA for 2 to 3 weeks and sections taken for hematoxylin & eosin (H&E) or reticulin staining. Images were taken using Olympus BX51 microscope with a Pixera 600ES camera using Viewfinder Version 3.01 (Pixera Corporation, San Jose, USA) software for image acquisition.

Flow cytometric analysis

Single cell suspensions from bone marrow and spleen were treated with ammonium chloride (STEMCELL Technologies, Vancouver, Canada) to remove red blood cells. Bone marrow (BM) and spleen (SP) mononuclear cells (MNCs) were stained with Ly6g Pacific Blue and Mac1 FITC (BioLegend, San Diego, USA) for myeloid; CD71 PE/Cy7 and Ter119 APC (BioLegend) for erythroid; and B220 APC and CD3e PE (BioLegend) for lymphoid analysis. For megakaryocytic analysis, BMMNCs and SPMNCs were stained with CD41 FITC (BD Biosciences), CD61 PE and CD42d APC (BioLegend). For LT-HSC and MkP staining, BMMNCs and SPMNCs were stained with lineage cocktail AF700 (anti-mCD3, Ly6G/Ly6C, mCD11b, mCD45R (B220), mTer-119), Sca-1 BV605, c-Kit APC/Cy7, CD48 APC, CD150 PE/Cy7 (BioLegend) and CD41 FITC (BD Biosciences, San Jose, USA). For early myeloerythroid precursors such as PreGM, GMP, PreCFU-E, CFU-E, PreMegE and MkP, flow cytometric analysis was performed as described, with BMMNCs and SPMNCs stained with lineage cocktail AF700, c-Kit APC/Cy7, Sca-1 BV605, CD105 APC, CD16/32 PE, CD150 PE/Cy7 (BioLegend) and CD41 FITC (BD).[1] All flow cytometry was carried out using a Fortessa analyzer (BD Biosciences) and data were analyzed using FlowJo software (Tree Star, Ashland, USA).

Analysis of plasma THPO levels

Plasma was collected by spinning whole blood at 2000g for 20 minutes at 4°C. Plasma THPO levels were measured using the Quantikine Mouse THPO Immunoassay kit according to the manufacturer's instructions (R&D Systems).

Platelet response to agonists

Whole blood from the inferior vena cava was collected into acid citrate dextrose (111 mM glucose, 71 mM citric acid, 116 mM sodium citrate), and flow cytometry was used to measure P-selectin exposure on and fibrinogen binding to platelets following stimulation with the following agonists: collagen-related peptide (CRP), thrombin and ADP, as previously described.[2]

Isolation of E-SLAM HSCs

Single cell suspensions of BM from adult $CALR^{del/+}$ or littermate control mice were isolated from the femurs, tibiae and iliac crest, and red blood cells were lysed with ammonium chloride (STEMCELL Technologies). E-SLAM HSCs were isolated as described previously[3] using CD45 FITC (BD Biosciences), EPCR PE (STEMCELL Technologies), CD150 PE/Cy7 (BioLegend), and CD48 APC (Biolegend). Single E-SLAM HSCs ($CD45^+EPCR^+CD48^-CD150^+$) were isolated using a Becton Dickinson Influx sorter (BD Biosciences).

1. Pronk CJH, Bryder D. Immunophenotypic Identification of Early Myeloerythroid Development. *Methods Mol Biol*. 2018;1678:301-319.
2. Hobbs CM, Manning H, Bennett C, et al. JAK2V617F leads to intrinsic changes in platelet formation and reactivity in a knock-in mouse model of essential thrombocythemia. *Blood*. 2013;122(23):3787-3797.
3. Kent DG, Copley MR, Benz C, et al. Prospective isolation and molecular characterization of hematopoietic stem cells with durable self-renewal potential. *Blood*. 2009;113(25):6342-6350.